

RSC Advances



This is an *Accepted Manuscript*, which has been through the Royal Society of Chemistry peer review process and has been accepted for publication.

Accepted Manuscripts are published online shortly after acceptance, before technical editing, formatting and proof reading. Using this free service, authors can make their results available to the community, in citable form, before we publish the edited article. This *Accepted Manuscript* will be replaced by the edited, formatted and paginated article as soon as this is available.

You can find more information about *Accepted Manuscripts* in the [Information for Authors](#).

Please note that technical editing may introduce minor changes to the text and/or graphics, which may alter content. The journal's standard [Terms & Conditions](#) and the [Ethical guidelines](#) still apply. In no event shall the Royal Society of Chemistry be held responsible for any errors or omissions in this *Accepted Manuscript* or any consequences arising from the use of any information it contains.

ARTICLE

Direct visualization of microphase separation in block copoly(3-alkylthiophene)s

Cite this: DOI: 10.1039/x0xx00000x

Pieter Willot,^a Joan Teyssandier,^b Wouter Dujardin,^a Jinne Adisojoso,^b Steven De Feyter,^b David Moerman,^c Philippe Leclère,^c Roberto Lazzaroni^c and Guy Koeckelberghs^aReceived 00th January 2012,
Accepted 00th January 2012

DOI: 10.1039/x0xx00000x

www.rsc.org/

A poly(3-octylthiophene)-*block*-poly(3-butylthiophene) block copolymer was synthesized in a one-pot block copolymerization reaction, starting from a functional *o*-tolyl initiator in order to maximize A-B diblock copolymer formation. First, the composition of this block copolymer is extensively studied using gel permeation chromatography (GPC) and ¹H NMR measurements. A complete block copolymer formation is obtained with almost equal block length; B-A-B block copolymer contamination is shown to be very limited. In a second part, the self-assembly was analysed through differential scanning calorimetry (DSC), atomic force microscopy (AFM) and scanning tunnelling microscopy (STM) measurements, focusing on the microphase separation. A direct visualization of the different microphases can be obtained with STM.

Introduction

All-conjugated block copolymers are promising materials for application in organic electronics as they can combine and improve the properties of the different constituting blocks in one molecule.^{1,2} Moreover, they distinguish themselves from polymer blends through unique aspects such as intrinsic stability, self-assembly, microphase separation, etc.. The production of new all-conjugated block copolymers has been growing dramatically in the last years, because of the broadening insight in the controlled polymerization mechanisms which are being applied to an ever increasing number of conjugated monomer systems.^{3–23} The increased control over the polymerization allows for a much better control over the molecular and, also, supramolecular structure.^{13,24–28} Applied to block copolymers with sufficiently differing blocks, this can result in a control over the microscopic morphology which is created by the microphases of the constituting blocks. In turn, a thermodynamically stable morphology can significantly enhance the performance and lifetime of e.g. bulk heterojunction solar cells.²⁹ Of course, as the synthetic possibilities broaden, the implementation of accurate and reliable analytical techniques needs to keep pace. The microphase separation behavior of block copolymers is most often studied with X-ray diffraction techniques, differential scanning calorimetry (DSC), atomic force microscopy (AFM) and transmitting electron microscopy. These techniques give insight into different aspects of the morphology of the polymers. The X-ray diffraction techniques

such as (Grazing Incidence) Wide Angle X-ray Scattering ((GI)WAXS),^{24,26,30,31} Wide Angle X-ray Diffraction (WAXD),^{27,31} Small Angle X-ray Scattering (SAXS)³¹ and X-ray diffraction (XRD)^{28,31,32} can identify the presence of different crystalline microphases by correlating the different observed refraction signals with the different microphases and these refraction signals also give insight in the lattices and stacking distances. The obtained stacking distances can this way directly be correlated with the different microphases that are present. Also Differential Scanning Calorimetry (DSC) measurements are frequently used to confirm the presence of separate microphases.^{24,26–28,31,32} This is often reflected in the presence of different melting peaks, that are normally ascribed to different microphases in the block copolymer, with their own semi-crystallinity.^{24,31,32} Nevertheless, these techniques do not provide an actual *visualization* of the phase separation. Atomic Force Microscopy (AFM)^{24,27–29,31–34} and Scanning or Transmitting Electron Microscopy (SEM²⁹ or TEM^{25,31} respectively) images are recorded to reveal the structure down to the nanometer scale. These techniques are capable of visualizing the supramolecular morphology of the block copolymers. Different domains in the polymer film can often be identified and are generally tentatively ascribed to the two microphases which are present in the block copolymer.^{24,28} These techniques, however, do not provide information on the chemical nature of the different domains, therefore these domains cannot unambiguously be assigned to one of the constituting blocks.

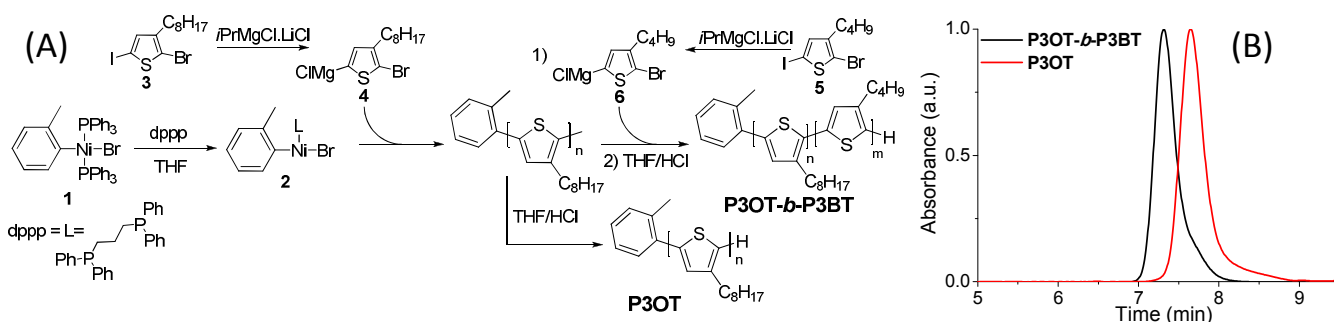


Figure 1. (A) Polymerization pathway in the synthesis of **P3OT** and **P3OT-*b*-P3BT**. (B) GPC elution curves of **P3OT** and **P3OT-*b*-P3BT**.

In order to extend the structural characterization to the molecular scale, Scanning Tunneling Microscopy (STM) is of prime interest as it is capable of imaging materials with sub-ångström resolution, also at the liquid-solid interface.³⁵ STM measurements have already been performed on several conjugated oligomers^{36–41} and polymers,^{42–44} including poly(3-alkylthiophene)s (P3AT).^{45–53} In those studies it has been demonstrated that molecularly resolved individual strands of regioregular P3AT can clearly be visualized and also that the length of the alkyl side-chains has a clearly marked influence on the chain-to-chain distance of the lamellae. Hence, STM could possibly be used to directly visualize the microphase separation. This type of information is of major importance in the analysis of microphase separation in block copolymers.

Microphase separation has been observed in an array of P3AT block copolymers with different combinations of side-chains. It has been found that microphase separation occurs if the difference in length of the alkyl chains between the blocks is more than 2 carbon atoms.³² In this work, we therefore consider a poly(3-octylthiophene)-*b*-poly(3-butylthiophene) (**P3OT-*b*-P3BT**) block copolymer, i.e., with an alkyl chain length difference of 4 carbon atoms, to ensure microphase separation and to enable an optimal study thereof.

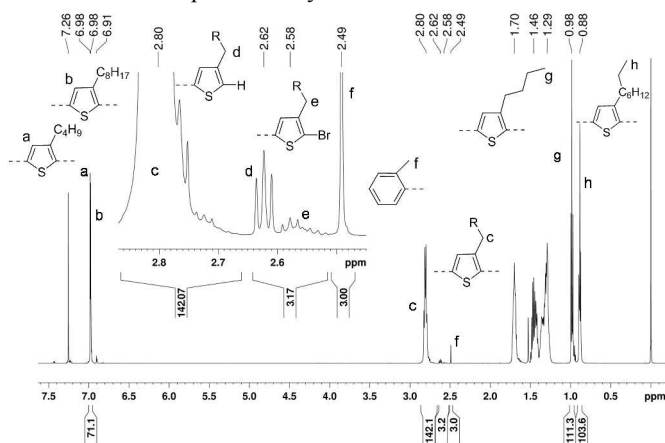


Figure 2. Interpretation of the ¹H NMR spectrum of **P3OT-*b*-P3BT**. The signals that are needed for the analysis of the chain-length and composition are assigned to the corresponding protons.

Results and Discussion

Polymer Synthesis

For poly(3-octylthiophene)-*b*-poly(3-butylthiophene), Wu *et al.* have already confirmed by DSC and X-ray studies that microphase separation occurs in this polymer, making it an ideal candidate for this study.³¹ The most straightforward synthetic approach towards this block copolymer is by using a Ni(dppp)-catalyzed Kumada Catalyst Transfer Protocol (KCTP) and forming the block copolymer by successive monomer addition in a one-pot polymerization.^{54,55} However, recent advances in this field have shown that the chain-walking of the Ni-catalyst over the polymer chain has a clear effect on the block copolymerization, leading to the formation of not only A-B diblock copolymers, but also a significant amount of B-A-B triblock copolymers.^{56,57} This results in ill-defined materials which are not ideal for further investigation of the microphase formation. To avoid these B-A-B contaminants as much as possible, a functional *o*-tolyl initiator is used, in order to maximize unidirectional growth and a preferential formation of the A-B block copolymer (Figure 1A).^{57,58}

The initiating entity (**2**) is formed from **1** through a ligand exchange with 2 eq. of diphenylphosphinopropane (dppp) after which a solution of the 3-octylthiophene monomer (**4**) is added. After a polymerization time of 1 hour, a part of the polymerization mixture is quenched with acidified THF to yield the homopolymer **P3OT**, while to the remainder, the 3-butylthiophene monomer (**6**) is added. After an additional block copolymerization time of 2 h, the block copolymer **P3OT-*b*-P3BT** is quenched with acidified THF, precipitated in MeOH and filtrated. Note that no longer reaction times were chosen to avoid disproportionation, which would result in undesired B-A-B triblock chains. The block copolymer is then further extracted with MeOH and CHCl₃ in a Soxhlet extraction to remove salts and catalyst residues. The CHCl₃-fraction is again precipitated in MeOH, filtered off and used for analysis. GPC analysis of the homopolymer **P3OT** and the block copolymer **P3OT-*b*-P3BT** shows a clear and complete shift from a \bar{M}_n -value of 9.3 kg/mol for **P3OT** to 14.5 kg/mol for **P3OT-*b*-P3BT** while the dispersity remains very low ($\bar{D} = 1.1$ for both polymers)(Figure 1B).

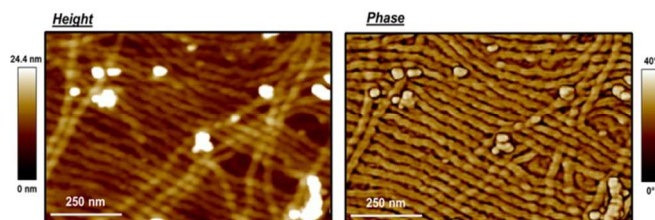
These results indicate the successful formation of the block copolymer. The structure of **P3OT-*b*-P3BT** is further analyzed using ^1H NMR spectroscopy to identify the composition of the block copolymer. The degree of polymerization can be calculated from the ^1H NMR spectrum, by comparing the relative integration values of signals corresponding to the different end groups with those of the repeating units. In Figure 2, all relevant signals have been assigned to the corresponding protons. These values are used in the chain length determination as described by Hardeman *et al.*:⁵⁹

$$DP = \frac{c}{\frac{d+e}{2} + \frac{f}{3}} + \frac{d+e}{\frac{d+e}{2} + \frac{f}{3}} = 56$$

A degree of polymerization of 56 units is found using this equation. Also note that the integration value of the aromatic signals at 6.98 ppm confirms this DP if they are scaled using the same method, corrected for the fact that the aromatic signal only corresponds to one proton per unit. This is also shown in the integration value, which equals half the integration value of signal c. If we then consider the ^1H NMR signals of the CH_3 -groups in the sidechains of both 3-butylthiophene (signal g) and 3-octylthiophene (signal h), the relative integration of 3-butylthiophene is 1.07 times higher than that of 3-octylthiophene. Considering also the total DP of 56 units, it can be concluded that the 3-octylthiophene block has a length of about 27 units and the 3-butylthiophene block consists of 29 units. Thorough analysis of the α -methylene region of the ^1H NMR spectrum (signals c-f) further indicates that $\pm 96\%$ of the polymer chains is indeed an A-B block copolymer, and that the amount of contaminants is limited (see Electronic Supplementary Information (ESI)).

Figure 3. Height (left) and phase (right) tapping-mode AFM image of a thin film of **P3OT-*b*-P3BT**.

Microphase separation study



With this understanding of the composition, the structural behavior of the block copolymer can be investigated. Differential scanning calorimetry (DSC) results of **P3OT-*b*-P3BT** are in line with previous results.³¹ Two melting transitions are observed: one broad signal at 163°C and one sharp peak at 252°C. The signal at 163°C can be ascribed to the P3OT block and the signal at 252°C to the P3BT block. During the cooling cycle, two corresponding crystallization peaks are also observed (Figures S3-4, ESI). The presence of two different melting transitions indicates that there is indeed microphase separation in the **P3OT-*b*-P3BT** block copolymer.

The morphological properties of the synthesized block copolymer are analyzed by AFM measurements to study the behavior in thin film. For this purpose, the block copolymer is dissolved in chlorobenzene and dropcasted onto an ITO-coated glass substrate. The solvent is evaporated overnight in a solvent-saturated atmosphere to favour self-assembly of the polymer chains. A representative image is depicted in Figure 3. A zoom is present in ESI (Figure S5) The AFM measurements clearly show the formation of a fibre-like morphology for the block copolymer. The width of the fibres is 26.1 ± 2.8 nm and they are several microns long. These results are very similar as in P3AT homopolymers.⁶⁰⁻⁶² Such a morphology is the result of the π - π stacking of polymer chains oriented perpendicular to the fiber axis. Note that the white spots probably correspond to aggregates due to the incomplete dissolution of the polymer, even after prolonged heating of the solutions at 60°C. There are no apparent features visible (e.g., the presence of an internal structure within the fibers) that could indicate microphase separation. This however does not imply the absence of phase separation, but may be simply due to the limited resolution of the AFM measurements at that scale. To obtain more insight into the microphase separation, we need to image this copolymer at a smaller scale. For that purpose, STM measurements of the **P3OT-*b*-P3BT** block copolymer were performed.

In order to study the morphology on highly ordered pyrolytic graphite (HOPG), a solution of **P3OT-*b*-P3BT** in 1,2,4-trichlorobenzene (TCB) with a concentration of 7.31×10^{-3} mg/mL is used to record *in situ* images at the HOPG-TCB interface. In these images, a sub-molecular resolution can be obtained, enabling the identification of individual thiophene units (Figure S6, ESI). A typical image at sub-monolayer coverage is shown in Figure 4a. In this image, individual strands of the block copolymer are visible. These strands are laterally stacked, as has been observed in previous measurements of P3ATs.⁴⁷ However, in case of the **P3OT-*b*-P3BT** block copolymer, the formation of two types of domains can clearly be observed, in which the lateral distance between the strands differs. These lateral distances have been evaluated by analysis of several series of images. The average value of the most dense domains (x) is 1.2 ± 0.1 nm, while the less dense domains (y) show a periodicity of 1.7 ± 0.1 nm. This difference in lateral distance can be correlated with the side-chain length in the two blocks. Indeed, previous reports showed an increasing lateral distance for longer side-chains.^{46,47,49,51,52} Taking this into account, the denser domains can be ascribed to the P3BT-block and the less dense domains are ascribed to the P3OT-block. These values correlate very well with the previously obtained values for hexyl and dodecyl side-chains (Figure 4b). From these values, we can tentatively establish a linear correlation between the side-chain length and the lateral stacking distance. These STM results clearly demonstrate that the two different blocks assemble only with blocks of the same nature and do not mix. This leads to the formation of nanometer-scale domains of each block, alternatively present

over the surface, *i.e.* microphase separation within the **P3OT-*b*-P3BT** block copolymer.

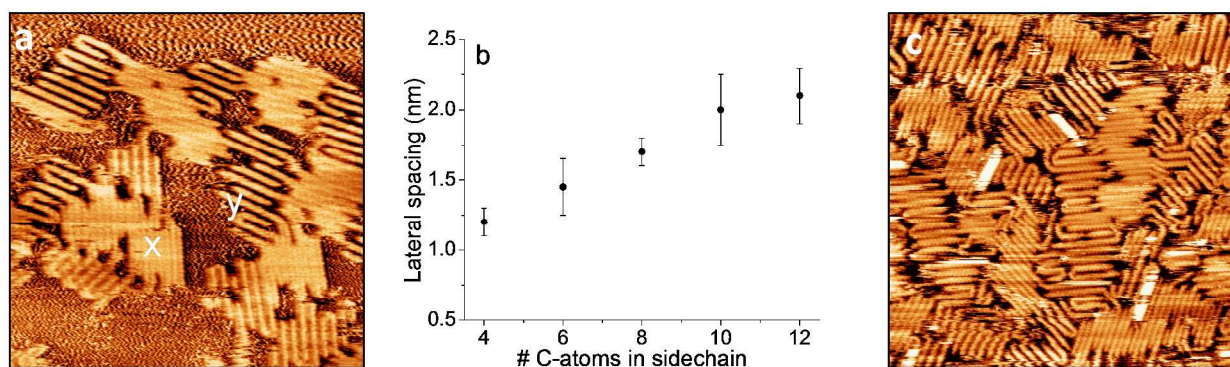


Figure 4. (a) STM-image recorded at a concentration of 7.31×10^{-3} mg/mL on HOPG ($60 \times 60 \text{ nm}^2$). The denser areas (x) are ascribed to the P3BT block and the less dense areas (y) to the P3OT block. Parameters of imaging: $I_t = 25 \text{ pA}$; $V_t = -1200 \text{ mV}$. (b) Linear correlation between lateral spacing of polymer strands and the number of carbon atoms in the side-chain. Values for hexyl, decyl and dodecyl side-chains are adapted from literature.^{46,47,49,51,52} (c) STM-image recorded at a concentration of 1.30×10^{-2} mg/mL on HOPG ($70 \times 70 \text{ nm}^2$). The brighter areas are polymer strands of the second layer. Parameters of imaging: $I_t = 300 \text{ pA}$; $V_t = -800 \text{ mV}$.

In Figure 4a, a sub-monolayer coverage is present. Further study of the formation of microphases can be performed at a higher surface coverage. This can be achieved by increasing the concentration of the solution. A representative image, recorded 105 min after dropcasting the original solution and equivalent with a concentration of 1.3×10^{-2} mg/mL due to evaporation, is shown in Figure 4c. This evidences that at full monolayer coverage, the same properties are maintained and different blocks exclusively assemble with themselves, resulting in microphase separation within the monolayer. Furthermore, chain-folding (hairpin bends within a polymer chain) can be observed in the monolayer. This chain-folding is frequently present in the P3OT-domains, but is seldom seen in the P3BT-domains even though the block lengths are very similar. This could be explained by the smaller folding radius expected in P3BT, which would cause more strain on the chain compared to P3OT, in which this folding radius is larger because of the larger lateral distance between the chains. The brighter areas in Figure 4c are ascribed to the presence of a second polymer layer. The assembly is, however, dynamic and slightly unstable, which can be observed with the ‘disappearance’ of some strands of the second layer in consecutive images, as well as reorganization in the first layer. However, from the images it is clear that the second layer consistently conserves the same orientation as the chains underneath. Furthermore, the high difference in contrast between the different layers shows that STM measurements can also be used for studying multilayers of polymers and the homogeneity of the films, and therefore the film-forming properties if higher concentrations are used (Figure S7, ESI). It is observed that also in the case of multilayers (>2), the upper layers conserve the orientation that is present in the first layer and that thicker films seem to be relatively homogenous since the difference between the highest

and the lowest topographic levels corresponds to the height of two layers.

Conclusions

In conclusion, a **P3OT-*b*-P3BT** block copolymer was synthesized with very little non-diblock copolymer impurities by successive monomer addition in a one-pot reaction using the Kumada Catalyst Transfer Protocol. ^1H NMR study showed a P3OT block length of 27 units and a P3BT block length of 29 with complete further growth and low Đ -values according to GPC. The self-assembling properties of **P3OT-*b*-P3BT** were studied using DSC and AFM measurements. Furthermore, the microphase separation in this block copolymer caused by the difference in the side-chain length in the two blocks was directly visualized by Scanning Tunneling Microscopy (STM). The different microphases could be assigned to the corresponding block by relating the lateral stacking distances between adjacent chains to the side-chain length of the polymer block. This allows to study the impact of molecular changes on the supramolecular structure, making STM a valuable tool towards further understanding and controlling microphase separation in conjugated block copolymers.

Acknowledgements

We are grateful to the Onderzoeksfonds KU Leuven/ Research Fund KU Leuven and the Fund for Scientific Research (FWO-Vlaanderen). PW is grateful to the agency for Innovation by Science and Technology (IWT) for a doctoral fellowship. JA thanks Fund for Scientific Research (FWO-Vlaanderen) for a postdoctoral fellowship. Part of the research leading to these results has also received funding from the European Research Council under the European Union’s Seventh Framework Programme (FP7/2007-2013)/ERC Grant Agreement no.

340324. The Leuven-Mons collaboration is supported by the Science Policy Office of the Belgian Federal Government (BELSPO - IAP 7/05). Research in Mons is also supported by the European Commission and Région Wallonne (FEDER program; SMARTFILM project) and FNRS/FRFC. D.M. is grateful to FRIA for a doctoral fellowship. Ph.L. is senior research associate of FNRS.

Notes and references

^a Laboratory for Polymer Synthesis, KU Leuven, Celestijnenlaan 200F, 3001 Leuven, Belgium.

^b Laboratory of Photochemistry and Spectroscopy, Division of Molecular Imaging and Photonics, KU Leuven, Celestijnenlaan 200F, 3001 Leuven, Belgium

^c Laboratory for Chemistry of Novel Materials, Center of Innovation and Research in Materials & Polymers (CIRMAP), University of Mons – UMONS/ Materia Nova, Place du Parc 20, B7000 Mons, Belgium

Electronic Supplementary Information (ESI) available: Experimental details, ¹H NMR spectra & calculations, DSC, AFM and STM results. See DOI: 10.1039/b000000x/

- U. Scherf, A. Gutacker, and N. Koenen, *Acc. Chem. Res.*, 2008, **41**, 1086–97.
- C. Guo, Y.-H. Lin, M. D. Witman, K. A. Smith, C. Wang, A. Hexemer, J. Strzalka, E. D. Gomez, and R. Verduzco, *Nano Lett.*, 2013, **13**, 2957–2963.
- M. C. Iovu, E. E. Sheina, R. R. Gil, and R. D. McCullough, *Macromolecules*, 2005, **38**, 8649–8656.
- T. Yokozawa, I. Adachi, R. Miyakoshi, and A. Yokoyama, *High Perform. Polym.*, 2007, **19**, 684–699.
- Y. Zhang, K. Tajima, K. Hirota, and K. Hashimoto, *J. Am. Chem. Soc.*, 2008, **130**, 7812–7813.
- K. Van den Bergh, J. Huybrechts, T. Verbiest, and G. Koeckelberghs, *Chem. Eur. J.*, 2008, **14**, 9122–9125.
- K. Van den Bergh, I. Cosemans, T. Verbiest, and G. Koeckelberghs, *Macromolecules*, 2010, **43**, 3794–3800.
- M. Verswyvel, K. Goossens, and G. Koeckelberghs, *Polym. Chem.*, 2013, **4**, 5310–5320.
- F. Boon, N. Hergué, G. Deshayes, D. Moerman, S. Desbief, J. De Winter, P. Gerbaux, Y. H. Geerts, R. Lazzaroni, and P. Dubois, *Polym. Chem.*, 2013, **4**, 4303–4307.
- Z. J. Bryan, M. L. Smith, and A. J. McNeil, *Macromol. Rapid Commun.*, 2012, **33**, 842–847.
- P. Willot, S. Govaerts, and G. Koeckelberghs, *Macromolecules*, 2013, **46**, 8888–8895.
- A. E. Javier, S. R. Varshney, and R. D. McCullough, *Macromolecules*, 2010, **43**, 3233–3237.
- J. Hollinger, A. A. Jahnke, N. Coombs, and D. S. Seferos, *J. Am. Chem. Soc.*, 2010, **132**, 8546–7.
- E. Goto, S. Nakamura, S. Kawauchi, H. Mori, M. Ueda, and T. Higashihara, *J. Polym. Sci. A Polym. Chem.*, 2014, **52**, 2287–2296.
- V. Senkovskyy, R. Tkachov, H. Komber, M. Sommer, M. Heuken, B. Voit, W. T. S. Huck, V. Kataev, A. Petr, and A. Kiriy, *J. Am. Chem. Soc.*, 2011, **133**, 19966–19970.
- Y. Nanashima, A. Yokoyama, and T. Yokozawa, *Macromolecules*, 2012, **45**, 2609–2613.
- A. Yokoyama, A. Kato, R. Miyakoshi, and T. Yokozawa, *Macromolecules*, 2008, **41**, 7271–7273.
- S. Wu, L. Bu, L. Huang, X. Yu, Y. Han, Y. Geng, and F. Wang, *Polymer*, 2009, **50**, 6245–6251.
- A. Amarjargal, L. D. Tijjing, C.-H. Park, I.-T. Im, and C. S. Kim, *Eur. Polym. J.*, 2013, **49**, 3796–3805.
- R. Miyakoshi, K. Shimono, A. Yokoyama, and T. Yokozawa, *J. Am. Chem. Soc.*, 2006, **128**, 16012–3.
- C. R. Bridges, H. Yan, A. A. Pollit, and D. S. Seferos, *ACS Macro Lett.*, 2014, **3**, 671–674.
- S. Wu, Y. Sun, L. Huang, J. Wang, Y. Zhou, Y. Geng, and F. Wang, *Macromolecules*, 2010, **43**, 4438–4440.
- A. Sui, X. Shi, S. Wu, H. Tian, Y. Geng, and F. Wang, *Macromolecules*, 2012, **45**, 5436–5443.
- R. Dattani, J. H. Bannock, Z. Fei, R. C. I. MacKenzie, A. A. Y. Guilbert, M. S. Vezie, J. Nelson, J. C. de Mello, M. Heeney, J. T. Cabral, and A. J. Nedoma, *J. Mater. Chem. A*, 2014, **2**, 14711.
- F. Li, K. G. Yager, N. M. Dawson, Y.-B. Jiang, K. J. Malloy, and Y. Qin, *Chem. Mater.*, 2014, **26**, 3747–3756.
- K. A. Smith, B. Stewart, K. G. Yager, J. Strzalka, and R. Verduzco, *J. Polym. Sci. B Polym. Phys.*, 2014, **52**, 900–906.
- J. Hollinger, P. M. DiCarmine, D. Karl, and D. S. Seferos, *Macromolecules*, 2012, **45**, 3772–3778.
- Y. Chen, H. Cui, L. Li, Z. Tian, and Z. Tang, *Polym. Chem.*, 2014, **5**, 4441–4445.
- H. Hoppe, M. Niggemann, C. Winder, J. Kraut, R. Hiesgen, A. Hinsch, D. Meissner, and N. S. Sariciftci, *Adv. Funct. Mater.*, 2004, **14**, 1005–1011.
- Y.-H. Lin, K. A. Smith, C. N. Kempf, and R. Verduzco, *Polym. Chem.*, 2013, **4**, 229–232.
- P.-T. Wu, G. Ren, C. Li, R. Mezzenga, and S. A. Jenekhe, *Macromolecules*, 2009, **42**, 2317–2320.
- J. Ge, M. He, F. Qiu, and Y. Yang, *Macromolecules*, 2010, **43**, 6422–6428.

33. P. Samori, M. Surin, V. Palermo, R. Lazzaroni, and P. Leclère, *Phys. Chem. Chem. Phys.*, 2006, **8**, 3927–3938.
34. L. Sardone, C. Sabatini, G. Latini, F. Barigelletti, G. Marletta, F. Cacialli, and P. Samor, *J. Mater. Chem.*, 2007, **17**, 1387–1391.
35. K. S. Mali, J. Adisojoso, E. Ghijsens, I. De Cat, and S. De Feyter, *Acc. Chem. Res.*, 2012, **45**, 1309–1320.
36. P. Samori, V. Francke, K. Müllen, and J. P. Rabe, *Chem. Eur. J.*, 1999, **5**, 2312–2317.
37. J.-R. Gong, H.-J. Yan, Q.-H. Yuan, L.-P. Xu, Z.-S. Bo, and L.-J. Wan, *J. Am. Chem. Soc.*, 2006, **128**, 12384–12385.
38. Q. Chen, T. Chen, X. Zhang, L.-J. Wan, H.-B. Liu, Y.-L. Li, and P. Stang, *Chem. Commun.*, 2009, 3765–3767.
39. S.-B. Lei, K. Deng, Y.-L. Yang, Q.-D. Zeng, C. Wang, Z. Ma, P. Wang, Y. Zhou, Q.-L. Fan, and W. Huang, *Macromolecules*, 2007, **40**, 4552–4560.
40. S. Lei, K. Deng, Z. Ma, W. Huang, and C. Wang, *Chem. Commun.*, 2011, **47**, 8829–8831.
41. A. Saywell, J. K. Sprafke, L. J. Esdaile, A. J. Britton, A. Rienzo, H. L. Anderson, J. N. O'Shea, and P. H. Beton, *Angew. Chem. Int. Ed.*, 2010, **49**, 9136–9.
42. Y. Okawa and M. Aono, *Nature*, 2001, **409**, 683–684.
43. L. Grill, M. Dyer, L. Laffrentz, M. Persson, M. V Peters, and S. Hecht, *Nat. Nanotechnol.*, 2007, **2**, 687–691.
44. D. F. Perepichka and F. Rosei, *Science*, 2009, **323**, 216–7.
45. L. Xu, L. Yang, and S. Lei, *Nanoscale*, 2012, **4**, 4399–415.
46. T. Kirschbaum, R. Azumi, E. Mena-Osteritz, and P. Bäuerle, *New J. Chem.*, 1999, **23**, 241–250.
47. E. Mena-Osteritz, A. Meyer, B. M. W. Langeveld-Voss, R. A. J. Janssen, E. W. Meijer, and P. Bäuerle, *Angew. Chem. Int. Ed.*, 2000, **39**, 2679–2684.
48. R. Azumi, G. Götz, T. Debaerdemaeker, and P. Bäuerle, *Chem. Eur. J.*, 2000, **6**, 735–744.
49. X. Ma, Y. Guo, T. Wang, and Z. Su, *J. Chem. Phys.*, 2013, **139**, 014701.
50. P. Keg, A. Lohani, D. Fichou, Y. M. Lam, Y. Wu, B. S. Ong, and S. G. Mhaisalkar, *Macromol. Rapid Commun.*, 2008, **29**, 1197–1202.
51. B. Grévin, P. Rannou, R. Payerne, A. Pron, and J. P. Travers, *J. Chem. Phys.*, 2003, **118**, 7097–7102.
52. A. Bocheux, I. Tahar-Djebbar, C. Fiorini-Debuisschert, L. Douillard, F. Mathevet, A.-J. Attias, and F. Charra, *Langmuir*, 2011, **27**, 10251–10255.
53. H. Peeters, P. Couturon, S. Vandeleene, D. Moerman, P. Leclère, R. Lazzaroni, I. De Cat, S. De Feyter, and G. Koeckelberghs, *RSC Adv.*, 2013, **3**, 3342.
54. E. E. Sheina, J. Liu, M. C. Iovu, D. W. Laird, and R. D. McCullough, *Macromolecules*, 2004, **37**, 3526–3528.
55. A. Yokoyama, R. Miyakoshi, and T. Yokozawa, *Macromolecules*, 2004, **37**, 1169–1171.
56. R. Tkachov, V. Senkovskyy, H. Komber, J.-U. Sommer, and A. Kiriy, *J. Am. Chem. Soc.*, 2010, **132**, 7803–7810.
57. M. Verswyvel, F. Monnaie, and G. Koeckelberghs, *Macromolecules*, 2011, **44**, 9489–9498.
58. A. Smeets, K. Van den Bergh, J. De Winter, P. Gerbaux, T. Verbiest, and G. Koeckelberghs, *Macromolecules*, 2009, **42**, 7638–7641.
59. T. Hardeman, P. Willot, J. De Winter, T. Josse, P. Gerbaux, P. Shestakova, E. Nies, and G. Koeckelberghs, *J. Polym. Sci. A Polym. Chem.*, 2014, **52**, 804–809.
60. G. Derue, S. Coppee, S. Gabriele, M. Surin, V. Geskin, F. Monteverde, P. Leclere, R. Lazzaroni, and P. Damman, *J. Am. Chem. Soc.*, 2005, **127**, 8018–8019.
61. M. Surin, P. Leclere, R. Lazzaroni, J. D. Yuen, G. Wang, D. Moses, A. J. Heeger, S. Cho, and K. Lee, *J. Appl. Phys.*, 2006, **100**, 033712/1–033712/6.
62. P. Willot, J. Steverlynck, D. Moerman, P. Leclère, R. Lazzaroni, and G. Koeckelberghs, *Polym. Chem.*, 2013, **4**, 2662–2671.

Graphical abstract

